Available online at www.sciencedirect.com
ScienceDirect
Biochimica et Biophysica Acta 1767 (2007) 233–243
Biochimica et Biophysica Acta
BBA
www.elsevier.com/locate/bbabio

Radiative and non-radiative charge recombination pathways in Photosystem II studied by thermoluminescence and chlorophyll fluorescence in the cyanobacterium *Synechocystis* 6803

Krisztián Cser, Imre Vass *

Institute of Plant Biology, Biological Research Center, Szeged, Hungary

Received 2 November 2006; received in revised form 30 December 2006; accepted 31 January 2007
Available online 7 February 2007

Abstract

The mechanism of charge recombination was studied in Photosystem II by using flash induced chlorophyll fluorescence and thermoluminescence measurements. The experiments were performed in intact cells of the cyanobacterium *Synechocystis* 6803 in which the redox properties of the primary pheophytin electron acceptor, Phe, the primary electron donor, P_{680}, and the first quinone electron acceptor, Q_A, were modified. In the D1Gln130Glu or D1His198Ala mutants, which shift the free energy of the primary radical pair to more positive values, charge recombination from the $S_2Q_A^-$ and $S_2Q_B^-$ states was accelerated relative to the wild type as shown by the faster decay of chlorophyll fluorescence yield, and the downshifted peak temperature of the thermoluminescence Q and B bands. The opposite effect, i.e. strong stabilization of charge recombination from both the $S_2Q_A^-$ and $S_2Q_B^-$ states was observed in the D1Gln130Leu or D1His198Lys mutants, which shift the free energy level of the primary radical pair to more negative values, as shown by the retarded decay of flash induced chlorophyll fluorescence and upshifted thermoluminescence peak temperatures. Importantly, these mutations caused a drastic change in the intensity of thermoluminescence, manifested by 8- and 22-fold increase in the D1Gln130Leu and D1His198Lys mutants, respectively, as well as by a 4- and 2.5-fold decrease in the D1Gln130Glu and D1His198Ala mutants, relative to the wild type, respectively. In the presence of the electron transport inhibitor bromoxynil, which decreases the redox potential of Q_A/Q_A^- relative to that observed in the presence of DCMU, charge recombination from the $S_2Q_A^-$ state was accelerated in the wild type and all mutant strains. Our data confirm that in PSII the dominant pathway of charge recombination goes through the $P_{680}^+Phe^-$ radical pair. This indirect recombination is branched into radiative and non-radiative pathways, which proceed via repopulation of P_{680}^* from $^1[P_{680}^+Ph^-]$ and direct recombination of the $^3[P_{680}^+Ph^-]$ and $^1[P_{680}^+Ph^-]$ radical states, respectively. An additional non-radiative pathway involves direct recombination of $P_{680}^+Q_A^-$. The yield of these charge recombination pathways is affected by the free energy gaps between the Photosystem II electron transfer components in a complex way: Increase of $\Delta G(P_{680}^* \leftrightarrow P_{680}^+Phe^-)$ decreases the yield of the indirect radiative pathway (in the 22–0.2% range). On the other hand, increase of ΔG $(P_{680}^+Phe^- \leftrightarrow P_{680}^+Q_A^-)$ increases the yield of the direct pathway (in the 2–50% range) and decreases the yield of the indirect non-radiative pathway (in the 97–37% range).

Keywords: Photosystem II; Charge recombination; Thermoluminescence; Flash-induced chlorophyll fluorescence

1. Introduction

Photosystem II is the redox active pigment–protein complex embedded in the thylakoid membrane that catalyses the oxidation of water and the reduction of plastoquinone. This catalytic function is performed by light driven electron transfer reactions through redox cofactors of the PSII reaction center. The initial photoact is charge separation between the excited reaction center chlorophyll (P_{680}) and the first acceptor, a pheophytin (Phe). The primary charge separated state,

Abbreviations: ADRY, Agents accelerating the Deactivation Reactions of the water splitting-enzyme Y; DCMU, 3-(3,4-dichlorophenyl)-1,1-dimethylurea; PSII, photosystem II; TL, thermoluminescence; WOC, water oxidation complex

* Corresponding author. Fax: +36 62 433 434.
E-mail address: imre@brc.hu (I. Vass).

0005-2728/$ - see front matter © 2007 Elsevier B.V. All rights reserved.
doi:10.1016/j.bbabio.2007.01.022

$P^+_{680}Phe^-$, is stabilized by secondary electron transfer reactions. On the acceptor side of PSII the electron is transferred from Phe^- to a permanently bound plastoquinone, called Q_A, in 200–400 ns, and Q_A^- is reoxidized by the second quinone electron acceptor called Q_B in 300–500 μs (see Ref. [1]). While Q_A is a firmly bound one-electron acceptor, Q_B can take up two electrons sequentially and leaves the binding site after forming the Q_BH_2 quinol state. On the donor side the first step of charge stabilization is the reduction of P^+_{680} by Y_Z. The final electron donor is the catalytic Mn cluster of water oxidation, which can exist in five oxidation states denoted as S_0,….,S_4 for recent reviews see [2–4].

Although PSII, as any other photosynthetic reaction center, is optimized for converting light energy into stabilized chemical energy the electron transfer reactions of PSII are reversible and the charge-separated states can be partly lost in charge recombination processes. These back reactions decrease the yield of the photosynthetic process and may function in the regulation of dissipating the excess light energy that can damage the reaction center complex [5,6]. Therefore, it is important to identify the different pathways of charge recombination and determine their efficiency. Charge recombination in PSII is a complex process, which involves back flow of electrons between secondary donors $S_{i+1}Tyr_ZP_{680} \leftrightarrow (S_iTyr_Z^{\bullet}P_{680} \leftrightarrow) S_iTyr_ZP^+_{680}$ and acceptors $Q_B^-Q_A \leftrightarrow Q_BQ_A^-$ (Scheme 1). From the $P^+_{680}Q_A^-$ state there are three different, radiative or non-radiative routes of charge recombination: (i) $P^+_{680}Q_A^-$ can recombine to the ground state via direct tunneling, which represents the direct non-radiative pathway. Experimental evidence for this pathway was provided by Reinmann and Mathis by showing that the rate of $P^+_{680}Q_A^-$ recombination is temperature independent below −70 °C and thermally activated between −70 and +20 °C [7]. The temperature independent process of $t_{1/2} \approx 1.7$ ms was assigned to direct recombination of $P^+_{680}Q_A^-$ to $P_{680}Q_A$ via tunneling. (ii) In a competing thermally activated process, back flow of electrons can restore the $P^+_{680}Phe^-$ radical state, either in the triplet or singlet spin configuration. The triplet radical pair will decay via the $^3[P^+_{680}Phe^-] \rightarrow {}^3P_{680}Phe$ pathway to the ground state ($\tau \approx 300$ ps, [8]). This process is non-radiative, since $^3P^*_{680}$ has only a very low yield of phosphorescence in the far-red region. The singlet radical pair can also contribute to the non-radiative decay process: if the lifetime of the $^1[P^+_{680}Phe^-]$ state is sufficiently long it can be converted to $^3[P^+_{680}Phe^-]$ via spin mixing in few ns [9]. In addition, the singlet radical pair can also decay via non-radiative direct recombination with a rate similar to that of spin mixing as shown by a recent theoretical calculation [10] (see also Ref. [11]), which is in agreement with previous experimental considerations (see Ref. [12]). These processes together represent the indirect non-radiative pathway of charge recombination. (iii) $^1[P^+_{680}Phe^-]$ can recombine to the $^1P^*_{680}Phe$ state, which decays via light emission and represents the indirect radiative pathway of charge recombination. Experimental evidence for the radiative pathway comes from the observation of delayed light emission (DLE) [12–14], which involves repopulation of the $^1[P^+_{680}Phe^-]$ singlet radical state and subsequent recombination to $^1P^*_{680}$ that decays to P_{680} via light emission. Further support is provided by the stimulation of DLE by temperature increase leading to thermoluminescence (TL) [15], and by transmembrane electric field leading to electro-luminescence [16–18].

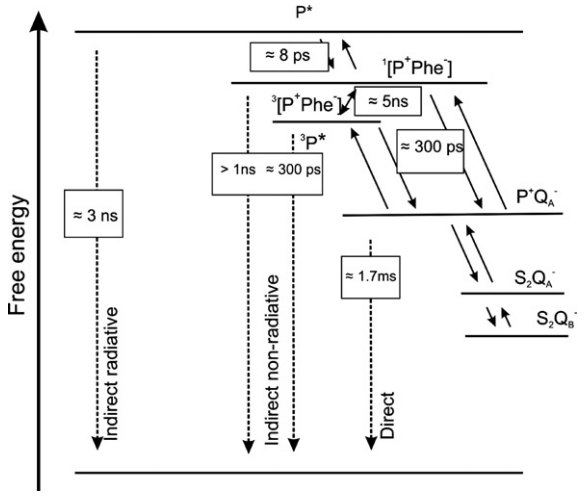

Scheme 1. Charge separation and charge recombination pathways in PSII. The solid arrows indicate electron transport processes, dashed arrows show the various charge recombination pathways with the respective time constants for the actual recombination (or dissipation) steps as described in the text.

The efficiency of the direct and indirect recombination pathways is expected to depend on the free energy levels of the participating redox components, especially of P_{680}, Phe and Q_A. In the reaction centers of purple bacteria, which have highly similar acceptor side as PSII, the increase of $\Delta G(BPhe \leftrightarrow Q_A)$ slows down the thermally activated recombination and favors the direct pathway, whereas the decrease of $\Delta G(BPhe \leftrightarrow Q_A)$ facilitates the indirect pathway [19–21], and similar effect is expected in PSII as well. The free energy level of Phe and P_{680} can be conveniently modified by site directed changes of amino acid residues in their environment. Mutation of D1Q130 to either Glu or Leu modifies the strength of hydrogen bond between this residue and Phe and changes the free energy level of the $P^+_{680}Phe^-$ state by +33 and −56 meV relative to the WT*, respectively [22]. Whereas, mutation of D1His198, located close to P_{680}, to either Ala or Gln changes the free energy level of the $P^+_{680}Phe^-$ state by +23 and −19 meV relative to the WT*, respectively [22]. In addition, the free energy level of Q_A is influenced by electron transport inhibitors that occupy the Q_B binding site [6,23]. Fluorescence relaxation measurements of the $S_2Q_A^-$ recombination showed acceleration of the recombination process in the D1Q130E strain, and the opposite effect was observed in the D1Q130L strain [24]. The recombination kinetics were also accelerated when the redox potential of Q_A was decreased in the presence of bromoxynil. These studies led to conclusion that the increase of the free energy gap between Phe and Q_A in the D1Q130L mutant slows down the indirect pathway to such an extent that recombination of the electron from Q_A^- proceeds predominantly via the direct $P^+_{680}Q_A^-$ tunneling pathway [24].

Changes in the free energy level of $P^+_{680}Phe^-$ due to modification of P_{680} also influence the kinetics of $S_2Q_A^-$ recombination, which is slowed down in the D1H198Q mutant,

and accelerated in the D1H198A mutant [25]. The effect of the D1His198 mutations on the direct and indirect charge recombination pathways has not been analyzed previously. However, correlated changes observed in the rate of $S_2Q_A^-$ recombination and in TL yield in different *Synechocystis* 6803 mutants affecting the lumenal CD-loop region of the D2 protein, that is expected to modify the P_{680} redox potential, were explained by changes in the yield of direct recombination [26]. Although the above cited reports agree on that non-radiative recombination pathways can be significant if the free energy levels of PSII electron transport components are modified, there is an apparent discrepancy in the interpretation of the experimental findings: Accelerated overall recombination kinetics were explained by both enhanced direct recombination [26] and indirect non-radiative recombination [24,27].

In order to obtain a better understanding of charge recombination pathways in PSII we performed comparative measurements of flash-induced chlorophyll fluorescence and thermoluminescence in D1Q130 and D1H198 mutants of *Synechocystis* 6803. Our results confirm that radiationless pathways dominate charge recombination in PSII, and show that the main route of the recombination process is the non-radiative indirect pathway that goes through the $[P_{680}^+Phe^-]$ radical state.

2. Materials and methods

Synechocystis sp. PCC 6803 cells were propagated in BG-11 growth medium in a rotary shaker at 30 °C under a 5% CO_2-enriched atmosphere. The intensity of white light during growth was 40 μE m^{-2} s^{-1}. Cells in the exponential growth phase (A_{580} of 0.8–1) were used. The D1Q130L (Q130L strain), D1Q130E (Q130E strain), D1H198A (H198A strain), and D1H198Q (H198Q strain) mutants were constructed in the *psb*A*3* gene of *Synechocystis* sp. PCC 6803 as described previously [28]. We also studied a photoautotrophic revertant of the originally photoheterotrophic D1H198K mutant, which carried no additional mutation in the D1 protein (H198K strain). The WT* used in this study is the TC35 strain, which was constructed in identical way as the mutants except that the transforming plasmid carried no site-directed mutation.

Thermoluminescence was measured with a home-built apparatus as in [29] on filter paper disks containing 50 μg Chl. Samples were preilluminated with continuous white light (10 Wm^{-2}) for 30 s and dark adapted for 3 min at +30 °C. Thermoluminescence was exited by a single turnover saturating flash either at +5 °C or −20 °C as indicated in the text. TL curves were usually recorded with 20 °C/min heating rate, with the exception of the heating rate series when 5 to 60 °C/min rates were used as indicated in the text.

Flash-Induced Fluorescence Relaxation Kinetics. Flash-induced increase and the subsequent decay of chlorophyll fluorescence yield were measured by a double-modulation fluorometer (PSI Instruments, Brno) [30] in the 150 μs to 100 s time range as described earlier [31]. The sample concentration was 5 μg Chl/ml. Multicomponent deconvolution of the measured curves was done by using a fitting function with three components. The fast and middle phases were simulated with exponential components. However, slow recombination of Q_A^- via charge recombination has been shown to obey hyperbolic kinetics corresponding to an apparently second order process [32]. Therefore, the slow phase was simulated with a hyperbolic component:

$$F(t) - F_0 = A_1\exp(-t/T_1) + A_2\exp(-t/T_2) + A_3/(-t/T_3)$$

where $F(t)$ is the variable fluorescence yield, F_0 is the basic fluorescence level before the flash, A_1–A_3 are the amplitudes, T_1–T_3 are the time constants. The non-linear correlation between fluorescence yield and the redox state of Q_A was corrected for using the Joliot model [33] with a value of 0.5 for the energy-transfer parameter between PS II units, which was obtained from the non-linear behavior of initial fluorescence amplitudes as a function of flash intensity.

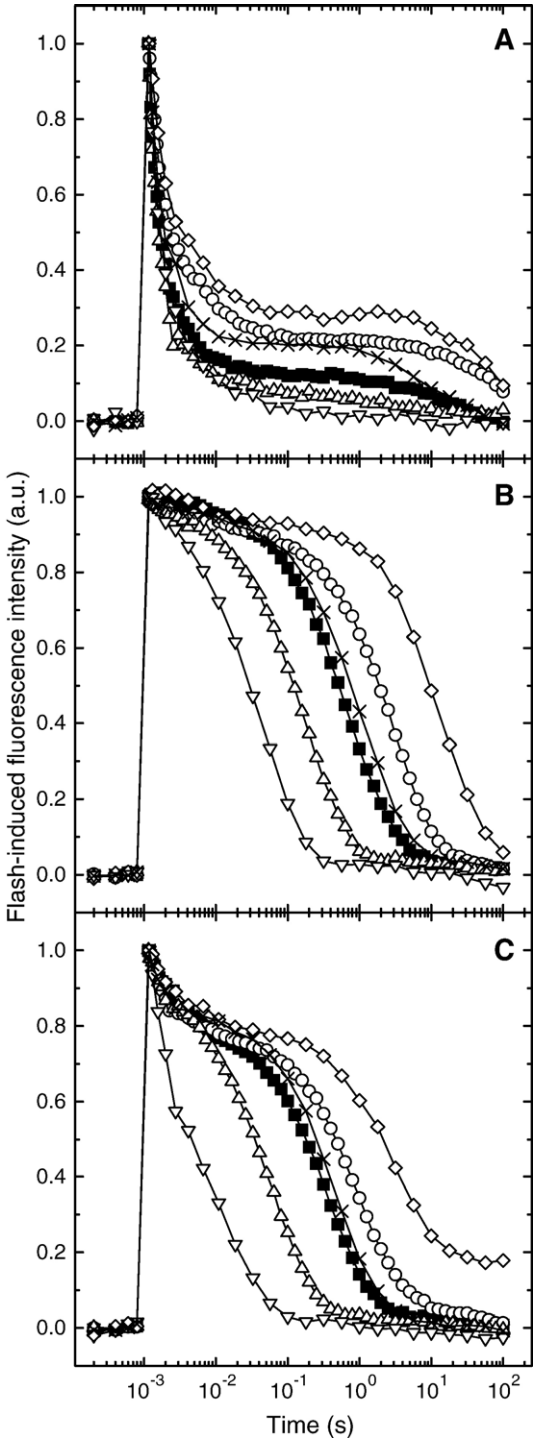

Fig. 1. Relaxation of flash induced chlorophyll fluorescence in the D1Q130 and D1H198 mutants. WT* (closed squares), Q130L (circles), Q130E (up triangles), H198Q (crosses), H198A (down triangles), H198K (diamonds) cells were excited with a single turnover saturating flash at $t=1$ ms. The measurements were performed in the absence of electron transport inhibitors (A), in the presence of 10 μM DCMU (B), and in the presence of 200 μM bromoxynil (C). The curves are shown after normalization to the same initial amplitude.

3. Results

3.1. Fluorescence decay in the absence of inhibitors

Illumination of *Synechocystis* 6803 cells with a single turnover saturating flash induces the reduction of Q_A, which leads to increased fluorescence yield. Subsequent reoxidation of Q_A^- in the dark results in the relaxation of fluorescence yield exhibiting three main decay phases, whose origin has been explained in the literature [34–36] as summarized below. The fast phase, which contributes to ~70% of the total decay with T_1 ~550 μs time constant in WT* cells (Fig. 1A and Table 1), arises from the reoxidation of Q_A^- by PQ molecules bound to the Q_B site before the flash. The middle phase, T_2 ~6 ms time constant and A_2 ~20% relative amplitude, originates from Q_A^- reoxidation by PQ molecules in centers where the Q_B site was empty at the time of the flash. Finally the slow phase, T_3 ~13 s time constant and A_3 ~10% relative amplitude, arises from back reaction of the S_2 state of the water-oxidizing complex with Q_A^-, which is populated via the equilibrium between $Q_A^-Q_B$ and $Q_AQ_B^-$. Although the D1Q130 and D1H198 residues are expected to influence primarily the redox properties of Phe and P_{680}, respectively, through changing the strength of H-bonding interaction the fluorescence decay curves measured in the absence of inhibitors reveal a significant effect on the rate of the Q_A to Q_B electron transfer (Fig. 1A, Table 1). The slower time constant of the fast phase in the Q130L, Q130E, H198K and H198Q mutants indicate slower oxidation of Q_A^- by bound Q_B.

Table 1
Time constants and relative amplitudes of the different phases of chlorophyll fluorescence relaxation in the D1Q130 and D1H198 mutants

Mutant	Fast phase T_1 (ms)/Amp (%)	Middle phase T_2 (ms)/Amp (%)	Slow phase T_3 (s)/Amp (%)
No addition			
WT*	0.55±0.07/69±2	6.2±0.8/22±1	13.3±2.3/9±0.1
Q130L	0.69±0.08/42±3	9.7±1.3/22±3	56.9±17/35±3.0
Q130E	0.63±0.01/73±4	9.1±1.9/17±2	2.4±0.7/10±0.1
H198K	0.69±0.04/35±3	9.5±1.6/24±2	76.1±12/41±3.5
H198A	0.68±0.03/72±3	8.0±1.4/18±2	3.1±0.6/10±0.2
H198Q	0.51±0.08/48±5	10.8±3.4/19±4	14.2±1.3/34±1.0
DCMU			
WT*	1.2±0.2/2.5±0.5	−(0)	1.05±0.06/97.5±1.9
Q130L	5.9±0.7/3.5±2	−(0)	4.7±0.11/96.5±2.6
Q130E	0.4±0.3/7.5±2	−(0)	0.22±0.04/92.5±2.1
H198K	5.1±0.6/3.9±1.8	−(0)	18.5±0.14/96.1±2.4
H198A	0.4±0.3/1.2±0.4	−(0)	0.05±0.04/98.8±1.8
H198Q	0.7±0.3/2.1±0.5	−(0)	1.45±0.06/97.9±1.5
Bromoxynil			
WT*	1.1±0.2/9.5±0.5	−(0)	0.42±0.06/90.5±1.0
Q130L	1.8±0.7/17.5±2	−(0)	1.85±0.14/82.5±2
Q130E	0.65±3/11±2	−(0)	0.09±0.04/89±2
H198K	6.5±0.8/8.7±2	−(0)	3.44±0.24/91.3±2
H198A	1.1±0.5/31±6	−(0)	0.02±0.01/69±3
H198Q	1.1±0.5/31±6	−(0)	0.672±0.01/69±3

The data were obtained from the analysis of the fluorescence relaxation curves as shown in Fig. 1 by using the function described in Materials and methods.

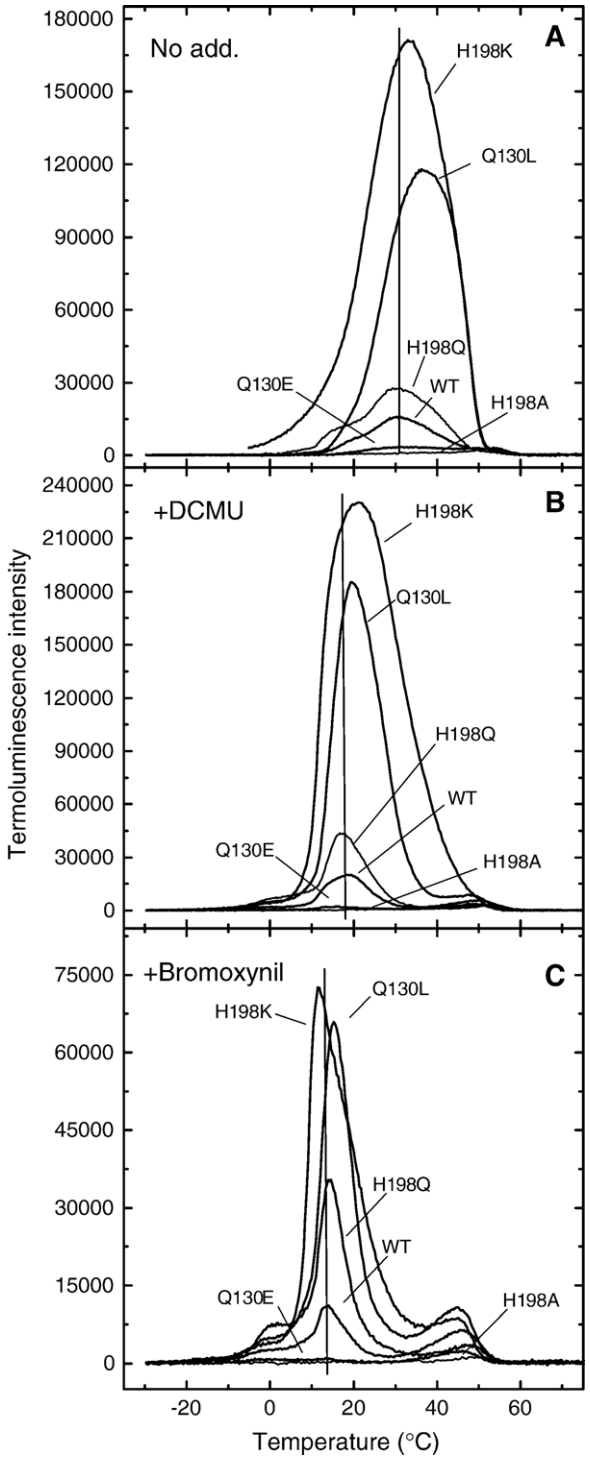

Fig. 2. Thermoluminescence characteristics of the D1Q130 and D1H198 mutants. WT*, Q130L, Q130E, H198A, H198Q and H198K cells were excited with a single turnover saturating flash at T=−20 °C. The measurements were performed in the absence of electron transport inhibitors (A), in the presence of 10 μM DCMU (B), and in the presence of 200 μM bromoxynil (C). Thermoluminescence was measured by using 20 °C/min heating rate.

This effect is accompanied by slower binding of PQ molecules from the pool to the Q_B site, as shown by the increased time constant of the middle phase. Together these findings point to a modification of the Q_B site in the mutants, which could be a

consequence of indirect structural changes induced by the amino acid replacements. In addition, the slow phase became slower and larger in H198Q and H198K, and accelerated in the Q130E and H198A mutants relative to the WT. Since the slow phase arises from the recombination of the S_2 state with Q_A^- via equilibrium with Q_B^- these changes are arising from the modified kinetics of the $S_2Q_A^-$ recombination as discussed below.

3.2. Fluorescence decay in the presence of inhibitors

When the Q_A to Q_B electron transfer step is blocked by DCMU, the reoxidation of Q_A^- proceeds via charge recombination with donor side components, mainly with the S_2 state. Modification of the $P_{680}^+Phe^-$ free energy level by mutating the D1Q130 and D1H198 residues has a profound effect on the fluorescence relaxation reflecting the $S_2Q_A^-$ recombination in the presence of DCMU. The fluorescence decay is accelerated when compared to the WT* in the DQ130E and H198A mutants in which the free energy of the $P_{680}^+Phe^-$ state is shifted to more positive values and the opposite effect is observed in the Q130L, H198Q, and H198K mutants in which the free energy of the $P_{680}^+Phe^-$ state is shifted to more negative values. These findings are in agreement with previous data obtained for the D1Q130 mutants in *Synechocystis* 6803 [24] and *Chlamydomonas reinhardtii* [37], as well as for the D1H198 mutants in *Synechocystis* 6803 [25].

The phenolic type inhibitor, bromoxynil shifts the free energy level of Q_A^- to more negative values than DCMU [6], therefore, destabilization of the $S_2Q_A^-$ recombination is expected. According to Fig. 1C, fluorescence relaxation is more complex in the presence of bromoxynil as in the presence of DCMU. The decay is biphasic showing a fast and slow phase. The fast phase most likely arises from the non-complete inhibition of the Q_A to Q_B electron transfer by the applied concentration of the inhibitor as indicated by oxygen evolution measurements (not shown), which could not be suppressed by further increase of bromoxynil concentration. Therefore, all measurements were performed at 200 μM bromoxynil and only the slow phase of fluorescence, which arises from the $S_2Q_A^-$ recombination, was evaluated. The slow phase of fluorescence decay is faster than that observed in the presence of DCMU in all the mutant strains.

3.3. Thermoluminescence characteristics

Fig. 2 shows the TL curves obtained in the absence and presence of electron transport inhibitors. After a single turnover flash the so-called B band is observed, which arises from the $S_2Q_B^-$ recombination [38,39] and appears at 31 °C in the WT* cells (Fig. 2A). In the Q130L, H198Q and H198K mutants the TL intensity was significantly increased, which was accompanied by the shift of the peak position to somewhat higher temperatures (Fig. 2A). The opposite effect was seen in the Q130E and H198A strains, in which the TL intensity drastically decreased, and its peak position somewhat down-shifted (Table 2). These data show that although the free energy level of the $P_{680}^+Phe^-$ state does not influence the total free energy gap between P_{680}^* and the charge storage state ($S_2Q_B^-$) it has a major influence on the TL yield.

In the presence of inhibitors of the Q_A to Q_B electron transfer step the main TL component arises from the $S_2Q_A^-$ recombination and designated as the Q band [38,40], which appears at around 19 °C in the WT* cells. The intensity of the Q band, when measured in the presence of DCMU, increased significantly in the H198Q strain and dramatically in the Q130L and H198K strains. In case of the Q130E and H198A mutants the intensity of the Q band was decreased (Fig. 2B). In the presence of DCMU another component, the so-called C band can be also be seen at around 50 °C, which arises from the $Y_D^{ox}Q_A^-$ recombination [41,42]. The studied mutations caused similar tendency change in the intensity of the C band as observed for the Q band, however the extent of the change was smaller.

When the Q_B site was blocked by the phenolic type inhibitor bromoxynil the peak position of the Q band was down shifted and its intensity decreased relative to that seen in the presence of DCMU. This effect was observed in all five strains supporting the results of fluorescence measurements that bromoxynil accelerates the $S_2Q_A^-$ recombination not only in the WT* and Q130E, H198A, but also in the Q130L, H198Q, and H198K strains.

Table 2
Peak temperatures and relative intensities of TL bands in the D1Q130 and D1H198 mutants

	Q band ($S_2Q_A^-$) DCMU		Q band ($S_2Q_A^-$) bromoxynil		B band ($S_2Q_B^-$)	
	T_m (°C)	Int[a]	T_m (°C)	Int[b]	T_m (°C)	Int[a]
WT*	19±0.8	1.0	14±0.7	0.30±0.03	31±0.7	1.0
Q130L	20±0.6	8.0± 0.5	16±0.6	1.2±0.1	36±0.8	8.0±0.4
Q130E	15±0.8	0.23±0.02	13±0.9	0.1±0.01	30±0.8	0.31±0.02
H198K	22±0.6	22.5±1.6	12±0.8	2.3±0.15	33±0.6	20.2±1.4
H198A	21±0.9	0.41±0.03	13±0.9	0.06±0.007	32±0.7	0.44±0.03
H198Q	17±0.8	2.62±0.2	14±0.8	0.81±0.05	31±0.9	2.46±0.2

TL was measured as in Fig. 2. in cell suspensions containing the same Chl concentration (40 μg Chl/sample), and the intensities were obtained by calculating the area under the respective peaks. Variations in the amount of functional PSII centers were taken into consideration by normalization of TL intensities to identical initial amplitudes of flash induced chlorophyll fluorescence transients measured in the presence of DCMU in the same strain.

[a] For the B band and Q bands the intensities are given after additional normalization to the values of the same TL band obtained in the WT* cells.

[b] For the Q band measured in the presence of bromoxynil the relative intensities are given after additional normalization to the intensity of the Q band obtained in the WT* cells in the presence of DCMU.

3.4. The effect of heating rate on the TL curves

TL measurements are performed at constant heating rate, which is usually around 20 °C/min. In the ideal case, when charge recombination proceeds exclusively via the indirect radiative pathway the same number of photons should be emitted at all heating rates for a given TL band. The cumulative photon emission (I_{tot}) is proportional to the time integral of TL intensity, which can be obtained by dividing the temperature-integrated TL intensity with the heating rate:

$$I_{tot} = c \int I(t)\mathrm{d}t = c/\beta \int I(T)\mathrm{d}T, \quad (1)$$

where I_{tot} is the cumulative photon emission, $I(t)$ and $I(T)$ are the TL intensities as a function of time and temperature, respectively; c is a proportionality constant; and β is the heating rate. According to Eq. (1), I_{tot} should be constant and the temperature-integrated TL intensity should increase linearly with increasing heating rates. Any deviation of I_{tot} from the constant value, or of the temperature-integrated TL intensity from linear increase, indicates the presence of non-radiative recombination pathways.

As shown by the data in Fig. 3A the intensity of the Q band is strongly increased with increasing heating rate in WT* cells. At the same time the peak position is shifted to higher temperatures. The intensity change comes partly from the change of the time window of TL emission when the heating rate is changed, i.e. TL photons are emitted during shorter time interval when the heating rate is increased, which leads to higher intensity when plotted as a function of temperature (see Eq. (1)). The up-shift of the peak position directly follows from the theoretical description of TL, since it depends on the ratio of the so-called pre-exponential factor of the recombination rate constant and of the heating rate [43,44]. If the constant factor is small higher temperatures are required to increase the overall recombination rate via the Boltzmann factor to values which permit efficient radiative recombination, and the TL signal appears at higher temperatures. Thus, the apparent decrease of the recombination rate due to division by increasing heating rates shifts the TL band to higher temperatures. Fig. 3B shows that the time-integrated TL intensity (I_{tot}) values are not constant, but gradually increase with increasing heating rates both in the WT* and the mutants. This result demonstrates that non-radiative pathway(s) have a significant effect on the yield of TL emission. At low heating rates, when the charge separated state stays for relatively long time at lower temperatures the non-radiative recombination pathway(s) efficiently compete with the indirect radiative pathway. When the heating rate is high the sample is rapidly warmed to higher temperatures, where the radiative pathway becomes more competitive. The gradual increase of the time-integrated TL intensity with increasing heating rate indicates higher thermal barrier (activation free energy) for the radiative pathway as compared with the non-radiative pathway(s) [45]. Normalization of the curves to the values obtained at the highest applied heating rate (60 °C/min) reveals different kinetics for the different strains. In the Q130L, H198Q and H198K mutants the

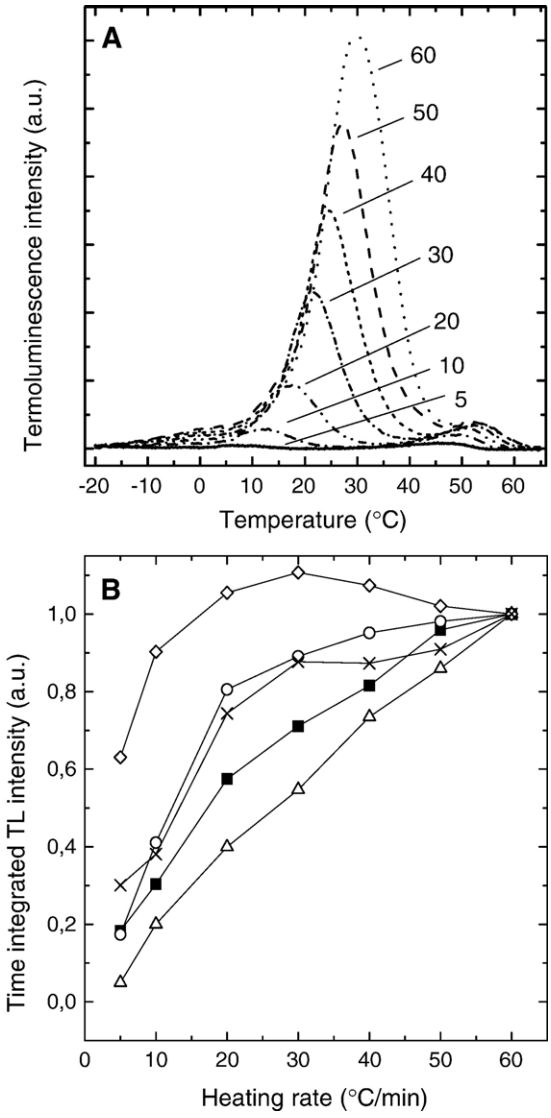

Fig. 3. The effect of heating rate on thermoluminescence. (A) WT* cells were treated with 10 μM DCMU and TL was measured after single flash excitation given at −20 °C by using 5, 10, 20, 30, 40, 50 and 60 °C/min heating rate as indicated in the figure. (B) TL curves were measured at different heating rates as in panel A and time integrated TL intensities were calculated dividing the area under the TL curves with the respective heating rate. The time integrated intensities are plotted as a function of the heating rate after normalization to 1 at 60 °C/min for WT* (closed squares), Q130L (circles), Q130E cells (up triangles), H198Q (crosses) as well as in H198K cells (diamonds).

increase of I_{tot} starts at lower heating rates and saturation is reached earlier than in the WT*. In contrast, in Q130E the curve is more steep than in the WT*, and does not reach saturation even at 60 °C/min heating rate (Fig. 3B). We have to note that we could not perform this analysis in the H198A mutant due to the very low TL intensities.

4. Discussion

Specific mutations of the D1Q130 and D1H198 residues, together with electron transport inhibitors acting at the Q_B site induce changes in the free energy level of PSII redox components (Fig. 4A), which provide very useful possibilities

to study the yield of the different charge recombination pathways. These effects can be experimentally assessed by the combination of thermoluminescence, which reflects selectively the indirect radiative pathway, and flash-induced chlorophyll fluorescence, which reflects the sum of all (radiative and non-radiative) pathways.

4.1. The efficiency of indirect radiative charge recombination pathway is regulated by $\Delta G(P^*_{680} \leftrightarrow P^+_{680}Phe^-)$

TL arises from the indirect radiative charge recombination pathway. Thus, TL intensity reflects the probability that the P^*_{680} state is repopulated, which in a simple model is expected to depend primarily on the amount of stabilized charge pairs

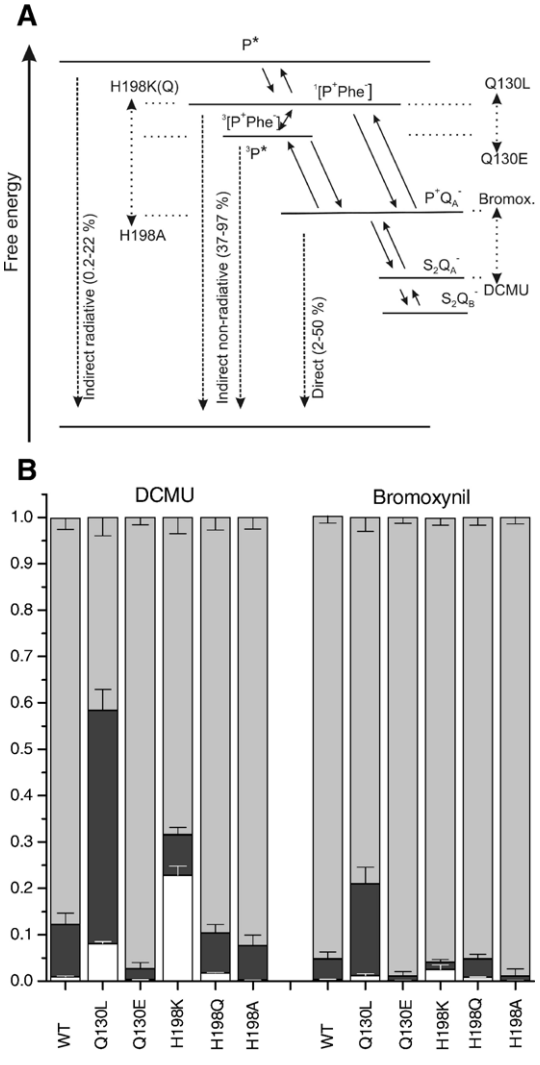

Fig. 4. Effects of D1Q130 and D1H198 mutations, and Q_B site inhibitors on the redox potentials and recombination yields in PSII. (A) Scheme of charge recombination pathways in which the double headed dotted arrows show the direction of free energy changes induced by the mutations or inhibitors. The ranges of charge recombination yields for the different pathways in the studied mutants, as calculated in panel B, are also shown. (B) The values for the yields of the direct (gray), indirect non-radiative (light gray) and indirect radiative (white) recombination routes were calculated from the measured fluorescence decay times and TL intensities as described in the text.

[44]. If charge recombination would proceed exclusively via the radiative pathway the same amount of photons should be emitted independent of the heating rate. Our data show that this is clearly not the case (Fig. 3B), and the pronounced dependence of the time integrated TL intensity on the heating rate demonstrates the significant effect of non-radiative processes on TL emission. The large variation of TL intensity shows that the efficiency of the non-radiative processes is suppressed in the Q130L and H198Q, as well as in the H198K strains and the opposite effect takes place in the Q130E strain. Similar effect is expected in the H198A mutant as well. However, the very weak TL signal did not permit reliable measurement of the heating rate dependence. In addition, the faster increase of I_{tot} with the heating rate in Q130L, H198Q and H198K indicates that the difference between the energy barriers for the radiative pathway and the overall non-radiative pathways is decreased in the Q130L, H198Q and H198K mutants, and increased in the Q130E mutant, respectively.

The strong modulation of TL intensity by the studied mutations, which affect the energetics of Phe or P_{680} demonstrates that the free-energy difference between P^*_{680} and $P^+_{680}Phe^-$ is an important regulatory factor of TL emission in agreement previous results [24]. It has to be noted that any possible effect of the mutations on the efficiency of charge stabilization in the $S_2Q_A^-$ or $S_2Q_B^-$ states has been eliminated by normalization of TL intensities to identical amount of stabilized charge pairs by using the initial amplitude of flash-induced chlorophyll fluorescence in the presence of DCMU.

The dependence of TL intensity on the free energy level of the primary radical pair is related to the rate of the $^1[P^+_{680}Phe^-] \rightarrow P^*_{680}$ Phe recombination relative to those of the alternative decay routes, i.e. spin mixing to $^3[P^+Phe^-]$, non-radiative recombination from the $^1[P^+Phe^-]$ state, and re-occurring charge separation that restores the $P^+_{680}Q_A^-$ state. The recombination rate of $^1[P^+_{680}Phe^-]$ to $^1P^*_{680}$ depends on the free energy gap between the radical pair and P^*_{680}. When either E_m (Phe/Phe^-) or $E_m(P^+_{680}/P_{680})$ is shifted to more negative values as in the case of the Q130L or H198Q and H198K mutants, respectively, the free energy gap decreases, and consequently the recombination rate increases. This effect increases the probability of P^*_{680} formation and facilitates the indirect radiative pathway, which is manifested by the increased yield of TL emission. In contrast to the above situation the shift of E_m(Phe/Phe^-) or $E_m(P^+_{680}/P_{680})$ to more positive values, as occurs in the case of the Q130E and H198A mutants, respectively, increases the free energy gap. Thus, the recombination rate of $^1[P^+_{680}Phe]$ to P^*_{680} will be decreased, and the probability of non-radiative recombination to the ground state, or re-separation to the $P^+_{680}Q_A^-$ state will increase.

As discussed above an important regulatory factor of TL intensity is $\Delta G(P^*_{680} \leftrightarrow P^+_{680}Phe^-)$. Assuming thermal equilibrium between these two states during TL emission the change of the free-energy gap induced by the Q130 and H198 mutations can be calculated from the relative TL intensities of the respective mutants. This calculation gives about 53, 23−25, and 77−80 meV decrease of $\Delta G(P^*_{680} \leftrightarrow P^+_{680}Phe^-)$ in the Q130L, H198Q, and

H198K mutants, respectively. Whereas, 30–38 and 28–30 mV increase is obtained in Q130E and the H198A mutants, respectively (Table 3). These values are very close to those obtained in isolated PSII cores of the same mutants by fast optical methods [22,46], and provide strong support for our approach. Our results are also in good agreement with the estimation of the redox potential change of P_{680} in whole cells of the H198K and H198Q mutants from flash induced chlorophyll fluorescence measurements [25]. In case of the H198A mutant the previous study resulted in a larger change of $E_m(P^+_{680}/P_{680})$ [25] then observed by us and in Ref. [22] (Table. 3), which might be due to different culturing conditions. The decrease of TL intensity in the presence of bromoxynil, which decreases $E_m(Q_A/Q_A^-)$ without affecting $E_m(\mathrm{Phe}/\mathrm{Phe}^-)$, is most likely related to the so called ADRY effect of phenolic type inhibitors, which accelerates the decay of the S-states without affecting their recombination rate.

In the simple model of TL, the peak position is determined by the free energy gap between P^*_{680} and $S_2Q_A^-$ (or $S_2Q_B^-$) [44,47], which is not affected significantly by the mutations. This model was further developed recently by Rappaport et al. who proposed that the change in the TL peak positions observed in *C. reinhardtii* mutants with Glu and Leu residues in the 130 position of the D1 protein can be explained by the assumption that the rate limiting step of TL emission is the repopulation of the $P^+_{680}\mathrm{Phe}^-$ state, from which P^*_{680} is formed in a recombination process whose free energy gap is much smaller than those of the previous steps and does not affect significantly the peak temperature [27]. Our data in *Synechocystis* 6803 are in complete agreement with these previous findings and show that the peak temperature of thermoluminescence is determined by the free energy gap between $P^+_{680}\mathrm{Phe}^-$ and $S_2Q_A^-$ (or $S_2Q_B^-$ in the absence of Q_B site inhibitors).

4.2. The overall rate of charge recombination is determined by $\Delta G(P^+_{680}\mathrm{Phe}^- \leftrightarrow S_2\,Q_A^-(Q_B^-))$

The overall charge recombination rate from the $S_2Q_A^-$ state is determined by the sum of the radiative and non-radiative processes, which can be conveniently measured by following the relaxation kinetics of flash-induced chlorophyll fluorescence. The kinetics of this process are strongly retarded by the Q130L, H198Q and H198K mutants (Fig. 1B), which have been shown to decrease the free energy level of $P^+_{680}\mathrm{Phe}^-$ [22,46], and the opposite effect was obtained in the Q130E and H198A mutants, which increase the free energy level of $P^+_{680}\mathrm{Phe}^-$. A straightforward explanation of these data is the modulation of the total free energy difference between the $S_2Q_A^-$ and $P^+_{680}\mathrm{Phe}^-$ states, which should be overcome by a thermally activated process if charge recombination proceeds via the indirect non-radiative pathway.

In the absence of inhibitors the slow phase of fluorescence decay arises from the recombination of the S_2 state with Q_B^- via the $Q_A^-Q_B \leftrightarrow Q_AQ_B^-$ equilibrium [35]. Therefore, the changing time constant of the slow phase, which increases in Q130L, H198Q and H198K, and decreases in Q130E and H198A relative to the WT*, can be explained by the changing free energy gap between $P^+_{680}\mathrm{Phe}^-$ and $S_2Q_B^-$ in the same way as described above for the $S_2Q_A^-$ recombination.

A previous analysis of fluorescence decay in the Q130L and Q130E mutants has led to the conclusion that due to the increase of the free energy gap between Phe and Q_A the rate of thermally activated indirect recombination pathway was slowed than to such an extent that the decay proceeds entirely via the direct recombination pathway, and thus the direct route has 100% efficiency in the Q130L mutant [24]. The main support for this idea was the observation that bromoxynil, a phenolic type inhibitor, which decreases $\Delta G(\mathrm{Phe}\leftrightarrow Q_A)$ by shifting $E_m(Q_A/Q_A^-)$ to more negative values than DCMU [6] accelerates the $S_2Q_A^-$ recombination in the WT* and Q130E, but not in Q130L strain. In contrast to these previous data, our fluorescence decay curves show the same, about 2-fold, acceleration of fluorescence decay in all strains, including Q130L in the presence of bromoxynil as compared to that in the presence of DCMU (Fig. 1 and Table 1). The destabilizing effect by bromoxynil was also confirmed by TL measurements, in the D1Q130L strain (Fig. 2). The reason for the discrepancy between our results and the previous literature data is not known at present, but the free energy shifts induced by bromoxynil relative to DCMU are rather consistently around 25 meV when calculated from the acceleration of fluorescence decay (Table 4). Therefore, although our results also show the significant decrease of the indirect pathway in the Q130L mutant (see discussion below), the earlier proposed complete suppression of the indirect route [24] is not justified by our fluorescence and TL data.

Table 3
Free energy changes related to charge recombination in the D1Q130 and D1H198 mutants

	$\Delta G(P^+_{680}\mathrm{Phe}^-)$ [a]		$\Delta G(P^+_{680}\mathrm{Phe}^-)$ [b]	$\Delta E(P^+_{680}/P_{680})$ [c]
	No addition (meV)	DCMU (meV)	No addition (meV)	DCMU (meV)
Q130L	52±3	52±3	56	
Q130E	−30±3	−38±4	−33	
H198K	77±3	80±4	80	88
H198Q	21±4	23±4	19	53
H198A	−28±4	−30±4	−23	−74

[a] The changes of free energy differences of the $S_2Q_A^-$ and $S_2Q_B^-$ recombinations in the mutants relative to the WT* were calculated from the relative intensity of the TL bands, shown in Table 2., as $\Delta(\Delta G)=kT\ \ln(TL_{int,\ mutant}/TL_{int,\ WT*})$. For comparison we also show data available in the literature in columns 4 and 5.

[b] Free energy changes of the primary radical pair estimated from fast transient absorption measurements at 60 ps after the excitation [22].

[c] Redox potential change of P^+_{680}/P_{680} estimated from the decay rate of flash induced chlorophyll fluorescence [25].

4.3. The efficiency of the different charge recombination routes

The overall rate constant of the $S_2Q_A^-$ recombination in WT cells is given by

$$k_{WT} = k_d + k_{id,WT}, \quad (2)$$

where k_d and $k_{id,WT}$ stands for the rate constants of the direct and indirect routes, respectively. Although the indirect process contains both the radiative and the non-radiative components, their rates are not separated here for the sake of simplicity. In the

Table 4
Free energy changes of the $S_2Q_A^-$ charge recombination induced by bromoxynil in the D1Q130 and D1H198 mutants

	$\Delta(\Delta G(P_{680}^+ \leftrightarrow S_2Q_A^-)$ (meV)
WT* (DCMU ↔ Bromox.)	23±5
Q130L (DCMU ↔ Bromox.)	24±4
Q130E (DCMU ↔ Bromox.)	23±5
H198K (DCMU ↔ Bromox.)	43±7
H198Q (DCMU ↔ Bromox.)	20±1
H198A (DCMU ↔ Bromox.)	24±3

The free energy difference of the $S_2Q_A^-$ recombination in the presence of DCMU and bromoxynil was calculated from the time constant of the slow phase of fluorescence decay, shown in Table 1, as $\Delta(\Delta G)=kT\ \ln(T_{3\text{bromoxynil}}/T_{3\text{DCMU}})$.

Q130 mutants as well as in the presence of Q_B site inhibitors, which affect the free energy gap between $P_{680}^+Phe^-$ and $P_{680}^+Q_A^-$ the recombination rate is

$$k_1 = k_d + k_{id,WT} \cdot e^{\Delta(\Delta G_{Phe,QA})/kT} \quad (3)$$

where $\Delta(\Delta G_{Phe,QA})$ is the change of the free energy gap between Phe and Q_A, relative to that in the WT PSII centers. Here it is assumed that mutations of the D1Q130 residue, or the presence of inhibitors do not induce structural changes of the PSII reaction center that would affect the direct recombination rate.

In the H198 mutants, which affect the free energy gap between $P_{680}^+Phe^-$ and $S_2Q_A^-$ the recombination rate is

$$k_2 = (k_d + k_{id,WT})e^{\Delta(\Delta G_{P680,S2})/kT} \quad (4)$$

where $\Delta(\Delta G_{P680,S2})$ is the change of the free energy gap between P_{680} and S_2, relative to that in the WT PSII centers.

By using the assumption that modifications of the Phe or Q_A free energy levels cause only negligible change in the rate of the direct recombination, $k_{d,WT}$ can be calculated from Eqs. (2), (3) and the overall recombination rates measured in the WT* and the Q130L strain as:

$$k_{d,WT} = \frac{k_1 - k_{WT} \cdot e^{\Delta(\Delta G_{Phe,QA})/kT}}{e^{\Delta(\Delta G_{Phe,QA})kT} - 1} \text{ and } k_{id,WT} = k_{WT} - k_{d,WT} \quad (5)$$

provided that a good estimation for $\Delta(\Delta G_{Phe,QA})$ is available. For that purpose we used the $\Delta G(P_{680}^+Phe^-) = -\Delta(\Delta G_{Phe,QA})$ values calculated from the intensity ratios of the thermoluminescence Q band in the WT and Q130L strains (Table 3). This assumption implies equilibrium conditions for the involved energy levels, which is expected to be fulfilled with good approximation for most of the involved energy levels. However, due to the very similar rates of forward electron transport and recombination to $^3P_{680}$ from the triplet radical pair only quasi equilibrium is expected between $^3[P_{680}^+Phe^-]$ and $P_{680}^+Q_A^-$, which might cause some decrease in the estimated change of the free energy gap between Q_A and Phe. It is also of note that in a previous work $k_{d,WT}$ was simply approximated by the overall recombination rate constant of $S_2Q_A^-$ in the Q130L strain [24]. However, this approximation was based on the apparent lack of effect of bromoxynil on the recombination kinetics in the Q130L strain, which observation we could not confirm. Therefore, we had to use the estimation of $k_{d,WT}$ described above. By this approach we obtained $k_{d,WT}=0.09$ in the presence of DCMU. Since modified redox potentials of Phe and Q_A are not expected to affect significantly the rate of the direct process the same $k_d=k_{d,WT}$ values were considered for the WT*, Q130L and the Q130E strain, as well as in the absence of inhibitors, or in the presence of bromoxynil. The yield of the direct process can be calculated as $\Phi_d=k_d/k_{WT}$, which gives 0.115–0.126 in the WT* in the presence of DCMU. Similar value (0.124) was obtained in the absence of DCMU, however, Φ_d decreased to 0.045 in the presence of bromoxynil (Fig. 4B). In the Q130 mutants Φ_d can be calculated as k_d/k_1 which resulted in 0.503 and 0.024 for the Q130L and Q130E strains, respectively in the presence of DCMU. Similar values were obtained by using the TL and fluorescence data measured in the absence of DCMU (0.532 and 0.022 for Q130L and Q130E, respectively). Whereas, the yield of the direct recombination route substantially decreased in the presence of bromoxynil (Φ_d=0.12 and 0.001 for the Q130L and Q130E strains, respectively, Fig. 4B). These data are in good qualitative agreement with the previous results of Rappaport et al. However, they estimated higher yield of the direct route by a factor of two (0.23 and 1 in the WT the Q130L mutant, respectively [24]) as a consequence of neglecting the indirect route in the Q130L strain.

Modification of the redox potential of P_{680} shifts the free energy level of both the $P_{680}^+Phe^-$ and $P_{680}^+Q_A^-$ states to the same extent and changes the overall recombination rate without affecting the ratio of the direct and indirect rates (Eq. (5)). Consequently, the H198 mutations do not change significantly the yield of the direct recombination pathway relative to the WT* cells.

The $P_{680}^+Q_A^-$ recombination in higher plant PSII has about 1.7 ms time constant below −70 °C, which is assigned to direct recombination via tunneling and agrees well with the 2 ms tunneling rate calculated from the PSII structure [10], whereas the time constant is 100–200 μs at room temperature [7]. If we assume that the rate of tunneling is approximately the same at room temperature as below −70 °C, the yield of the direct route should be around 0.06–0.12, which is in good agreement with our estimation of 0.115–0.126 in the WT *Synechocystis* 6803 cells. Considering further the about 240 meV free energy gap between the S_2 state and P_{680}^+ [24] together with the 1.7 ms for the tunneling rate [7] the overall direct recombination rate of $S_2Q_A^-$ can be estimated as 0.05 s^{-1} which is close to our 0.09–0.11 s^{-1} value and supports the reliability of our method.

For estimating the yield of the indirect radiative route we can make the assumption that light emission occurs only in the population of reaction centers in which the singlet radical pair is formed through the indirect pathway, i.e. considering the 3:1 ratio of the triplet : singlet population Φ_{exc} should not exceed 25% of the indirect yield. Assuming further that in the H198K mutant this upper limit is closely approached, the yield of the radiative process can be estimated as $\Phi_{exc}=0.25*(1-\Phi_d)\approx 0.22$ in the H198K strain. From the about 22-fold decrease of TL intensity in the WT* cells as compared to the H198K strain $\Phi_{exc}\approx 0{,}01$ is obtained (DCMU) −0,018 (no addition) in the

WT*, which is reasonably close to the 0,028 value estimated for higher plants from delayed light measurements [48].

It follows from the above considerations that the main route of charge recombination is the indirect non-radiative process whose yield is $\Phi_{id} \approx 0.86$ in the WT* Synechocystis cells in the absence of inhibitors. This yield is increased somewhat by DCMU (0.88) and by bromoxynil (0.95). The yield of the indirect route is further enhanced in the Q130E mutant, with $\Phi_{id} \approx 0{,}97–0{,}99$. However, in the Q130L mutant the indirect non-radiative pathway has only about 0.42 yield in the presence of DCMU and 0.37 without addition, which increases to about 0.79 in the presence of bromoxynil (Fig. 4B). It has to be noted that due to the assumption that the yield of the indirect radiative route in the H198K mutant represents the potential maximum, the Φ_{exc} values might be overestimated at the expense of the Φ_{id} values. However, this numerical uncertainty in the calculations does not affect the overall trend of the relative efficiency of the three recombination routes.

4.4. Physiological role

Our data show a remarkably flexible regulation of charge recombination pathways by the free energy gaps at the PSII acceptor side. Although natural mutations of the D1-H198 residue are not known, cyanobacteria often have 2–3 different D1 protein forms in the same cell, in which the 130th amino acid position is always occupied either by glutamine or glutamate. Under high light and other stress conditions the Glu containing D1 form replaces the Gln containing D1 form, as in the case of *Synecochoccus* 7942 [49] or *Anabeana* 7120 [50]. The D1 protein form exchange provides increased phototolerance to the cells [49], which is accompanied by accelerated non-radiative charge recombination [51]. During continuous illumination Q_A is reduced in a large fraction of the centers, which decreases the yield of primary radical pair formation, but does not prevent it completely. Elimination of the primary radical pair occurs via the competing pathways of radiative and direct non-radiative recombination of $^1[P^+_{680}Phe^-]$, as well as via its conversion to $^3[P^+_{680}Phe^-]$, which leads to the formation of potentially harmful $^3P_{680}$ through its singlet oxygen producing interaction with molecular oxygen. Therefore a photoprotective effect should involve enhanced probability for the non-radiative recombination of the singlet radical pair, which prevents $^3P_{680}$ formation. This possibility is supported by the observation of a 300 ps non-radiative dissipation of the singlet excited state observed in the Q130E mutant *Synechocystis* 6803 [22], which points to a possible regulatory mechanism of photo-tolerance in which the redox potential change of Phe regulates the harmless dissipation of excess light energy. Experimental verification of this hypothesis is currently in progress in our laboratory.

Acknowledgements

This work was supported by grants from European Union (MRTN-CT-2003-505069, and STREP-SOLAR-H-516510). The studied mutants were kindly provided by Dr. Peter Nixon, Imperial College. Useful discussion with Hans van Gorkom, William Rutherford and Fabrice Rappaport are appreciated.

References

[1] Ö. Hansson, T. Wydrzynski, Current perceptions of Photosystem II, Photosynth. Res. 23 (1990) 131–162.
[2] G. Renger, Photosynthetic water oxidation to molecular oxygen: apparatus and mechanism, Biochim. Biophys. Acta 1503 (2001) 210–228.
[3] J. Messinger, Towards understanding the chemistry of photosynthetic oxygen evolution: dynamic structural changes, redox states and substrate water binding of Mn cluster in Photosystem II, Biochim. Biophys. Acta 1459 (2000) 481–488.
[4] K. Sauer, V.K. Yachandra, The water-oxidation complex in photosynthesis, Biochim. Biophys. Acta 1655 (2004) 140–148.
[5] N. Keren, A. Berg, P.J.M. van Kan, H. Levanon, I. Ohad, Mechanism of photosystem II photoinactivation and D1 protein degradation at low light: the role of back electron flow, Proc. Natl. Acad. Sci. U. S. A. 94 (1997) 1579–1584.
[6] A. Krieger-Liszkay, A.W. Rutherford, Influence of herbicide binding on the redox potential of the quinone acceptor in photosystem II: relevance to photodamage and phytotoxicity, Biochemistry 37 (1998) 17339–17344.
[7] S. Reinman, P. Mathis, Influence of temperature on photosystem II electron transfer reactions, Biochim. Biophys. Acta 635 (1981) 249–258.
[8] M. Volk, M. Gilbert, G. Rousseau, M. Richter, A. Ogrodnik, M.E. Michel-Beyerle, Similarity of primary radical pair recombination in photosystem II and bacterial reaction centers, FEBS Lett. 336 (1993) 357–362.
[9] A.J. Hoff, Magnetic field effects on photosynthetic reactions, Q. Rev. Biophys. 14 (1981) 599–665.
[10] C.C. Moser, C.C. Page, P.L. Dutton, Tunneling in PSII, Photochem. Photobiol. Sci. 4 (2005) 933–939.
[11] M. Grabolle, H. Dau, Energetics of primary and secondary electron transfer in Photosystem II membrane particles of spinach revisited on basis of recombination-fluorescence measurements, Biochim. Biophys. Acta 1708 (2005) 209–218.
[12] H.J. van Gorkom, Electron transfer in photosystem II, Photosynth. Res. 6 (1985) 97–112.
[13] W. Arnold, H. Sherwood, Energy storage in chloroplasts, J. Phys. Chem. 63 (1959) 2–4.
[14] W. Arnold, Delayed light in photosynthesis, Annu. Rev. Biophys. Bioeng. 6 (1977) 1–6.
[15] W. Arnold, H.K. Sherwood, Are chloroplasts semiconductors? Proc. Natl. Acad. Sci. U. S. A. 43 (1957) 105–114.
[16] J.L. Ellenson, K. Sauer, The electrophotoluminescence of chloroplasts, Photochem. Photobiol. 23 (1976) 113–123.
[17] H.J. van Gorkom, R.F. Meiburg, R.J. van Dorssen, The Effects of an Electrical Field on the Primary Reactions of System II, in: C. Sybesma (Ed.), Advances in Photosynthesis Research, Martinus Nijhoff/Dr W. Junk Publishers, 1984, pp. 329–332.
[18] M.H. Vos, H.J. van Gorkom, P.J. van Leewen, An electroluminescence study of stabilization reactions in the oxygen-evolving complex of Photosystem II, Biochim. Biophys. Acta 1056 (1991) 27–39.
[19] A. Gopher, Y. Blatt, A. Schönfeld, M.Y. Okamura, G. Feher, M. Montal, The effect of an applied electric field on the charge recombination kinetics in reaction centers reconstituted in planar lipid bilayers, Biophys. J. 48 (1985) 311–320.
[20] N.W. Woodbury, W.W. Parson, M.R. Gunner, R.C. Prince, P.L. Dutton, Radical-pair energetics and decay mechanisms in reaction centers containing anthraquinones, naphthoquinones or benzoquinones in place of ubiquinone, Biochim. Biophys. Acta 851 (1986) 6–22.
[21] R.J. Shopes, C.A. Wraight, Charge recombination from $P^+Q^-_A$ state in reaction centers from *Rhodopseudomonas viridis*, Biochim. Biophys. Acta 893 (1987) 409–425.
[22] S.A.P. Merry, P.J. Nixon, L.M.C. Barter, M. Schilstra, G. Porter, J. Barber, Modulation of quantum yield of primary radical pair formation in

Photosystem II by site-directed mutagenesis affecting radical cations and anions, Biochemistry 37 (1998) 17439–17447.
[23] I. Vass, S. Demeter, Classification of photosystem II inhibitors by thermodynamic characterization of thermoluminescence of inhibitor-treated chloroplasts, Biochim. Biophys. Acta 682 (1982) 496–499.
[24] F. Rappaport, M. Guergova-Kuras, P.J. Nixon, B.A. Diner, J. Lavergne, Kinetics and pathways of charge recombination in photosystem II, Biochemistry 41 (2002) 8518–8527.
[25] B.A. Diner, E. Schlodder, P.J. Nixon, W.J. Coleman, F. Rappaport, J. Lavergne, W.F.J. Vermaas, D. Chisholm, Site-directed mutations at D1-His198 and D2-His197 of Photosystem II in *Synechocystis* PCC 6803: sites of primary charge separation an cation and triplet stabilization, Biochemistry 40 (2001) 9265–9281.
[26] D.V. Vavilin, W.F.J. Vermaas, Mutations in the CD-Loop region of the D2 Protein in *Synechocystis* sp. PCC 6803 modify charge recombination pathways in Photosystem II in vivo, Biochemistry 39 (2000) 14831–14838.
[27] F. Rappaport, A. Cuni, L. Xiong, R. Sayre, J. Lavergne, Charge recombination and thermoluminescence in Photosystem, Biophys. J. 88 (2005) 1948–1958.
[28] P.J. Nixon, T. Trost, B.A. Diner, Role of the carboxy terminus of polypeptide D1 in the assembly of a functional water-oxidizing manganese cluster in photosystem II of the cyanobacterium *Synechocystis* sp. PCC 6803: assembly requires a free carboxyl group at C-terminal position 344, Biochemistry 31 (1992) 10859–10871.
[29] I. Vass, K.M. Cook, Zs. Deák, S.R. Mayes, J. Barber, Thermoluminescence and flash-oxygen characterization of the IC2 deletion mutant of Synechocystis sp. PCC 6803 lacking the photosystem II 33 kDa protein, Biochim. Biophys. Acta 1102 (1992) 195–201.
[30] M. Trtilek, D.M. Kramer, M. Koblizek, Dual-modulation LED kinetic fluorometer, J. Lumin. 72–74 (1997) 597–599.
[31] I. Vass, D. Kirilovsky, A.-L. Etienne, UV-B radiation-induced donor- and acceptor-side modifications of Photosystem II in the cyanobacterium *Synechocystis* sp. PCC 6803, Biochemistry 38 (1999) 12786–12794.
[32] P. Bennoun, Chlororespiration revisited: mitochondrial-plastid intereaction in *Chlamydomonas*, Biochim. Biophys. Acta 1186 (1994) 59–66.
[33] A. Joliot, P. Joliot, Etude cinétique de la réaction photochimique libérant l'oxygéne au cours de la photosynthése, C. R. Acad. Sci. 258 (1964) 4622–4625.
[34] A.R. Crofts, C.A. Wraight, The electrochemical domain of photosynthesis, Biochim. Biophys. Acta 726 (1983) 149–185.
[35] G. Renger, H.-J. Eckert, A. Bergmann, J. Bernarding, B. Liu, A. Napiwotzki, F. Reifarth, H.-J. Eichler, Fluorescence and spectroscopic studies of exciton trapping and electron transfer in Photosystem II of higher plants, Aust. J. Plant Physiol. 22 (1995) 167–181.
[36] R. de Wijn, H.J. van Gorkom, Kinetics of electron transfer from Q_A to Q_B in Photosystem, Biochemistry 40 (2001) 11912–11922.
[37] A. Cuni, L. Xiong, R.T. Sayre, F. Rappaport, J. Lavergne, Modification of the pheophytin midpoint potential in photosystem II: modulation of the quantum yield of charge separation and of charge recombination pathways, Phys. Chem. Chem. Phys. 6 (2004) 4825–4831.
[38] A.W. Rutherford, A.R. Crofts, Y. Inoue, Thermoluminescence as a probe of photosystem II photochemistry: the origin of the flash-induced glow peaks, Biochim. Biophys. Acta 682 (1982) 457–465.
[39] S. Demeter, I. Vass, Charge accumulation and recombination in photosystem II studied by thermoluminescence. I. Participation of the primary acceptor Q and secondary acceptor B in the generation of thermoluminescence of chloroplasts, Biochim. Biophys. Acta 764 (1984) 24–32.
[40] M. Droppa, G. Horváth, I. Vass, S. Demeter, Mode of action of Photosystem II herbicides studied by thermoluminescence, Biochim. Biophys. Acta 638 (1981) 210–216.
[41] S. Demeter, C. Goussias, G. Bernát, L. Kovács, V. Petrouleas, Participation of the g=1.9 and g=1.82 EPR forms of the semiquinone–iron complex, $Q_A^-Fe^{2+}$ of photosystem II in the generation of the Q and C thermoluminescence bands, respectively, FEBS Lett. 336 (1993) 352–356.
[42] G.N. Johnson, A. Boussac, A.W. Rutherford, The origin of the 40–50 °C thermoluminescence bands in photosystem II, Biochim. Biophys. Acta 1184 (1994) 85–92.
[43] J.T. Randall, M.H.F. Wilkins, Phosphorescence and electron traps: I. The study of trap distributions, Proc. R. Soc. Lond., A 184 (1945) 366–369.
[44] I. Vass, G. Horvath, T. Herczeg, S. Demeter, Photosynthetic energy conservation investigated by thermoluminescence. Activation energies and half-lives of thermoluminescence bands of chloroplasts determined by mathematical resolution of glow curves, Biochim. Biophys. Acta 634 (1981) 140–152.
[45] I. Vass, S. Demeter, in: C. Sybesma (Ed.), Energetic Characterization of the Thermoluminescence in Isolated Chloroplasts, Martinus Nijhoff/Dr. W. Junk Publishers, The Hague, The Netherlands, 1984, pp. 737–740.
[46] L.B. Giorgi, P.J. Nixon, S.A.P. Merry, D.M. Joseph, J.R. Durrant, J. De Las Rivas, J. Barber, G. Porter, D.R. Klug, Comparison of primary charge separation in the Photosystem II reaction center complex isolated from wild-type and D1-130 mutants of the cyanobacterium *Synechocystis* PCC 6803, J. Biol. Chem. 271 (1996) 2093–2101.
[47] D. de Vault, Govindjee, W. Arnold, Energetics of photosynthetic glow peaks, Proc. Natl. Acad. Sci. U. S. A. 80 (1983) 983–987.
[48] B.G. de Grooth, H.J. van Gorkom, External electric field effects on prompt and delayed fluorescence in chloroplasts, Biochim. Biophys. Acta 635 (1981) 445–456.
[49] D. Campbell, G.Q. Zhou, P. Gustafsson, G. Oquist, A.K. Clarke, Electron transport regulates exchange of two forms of photosystem II D1 protein in the cyanobacterium *Synechococcus*, EMBO J. 14 (1995) 5457–5466.
[50] C. Sicora, S.E. Appleton, C.M. Brown, J. Chung, J. Chandler, A.M. Cockshutt, I. Vass, D.A. Campbell, Cyanobacterial *psbA* families in *Anabaena* and *Synechocystis* encode trace, constitutive and UVB-induced D1 isoforms, Biochim. Biophys. Acta 1757 (2006) 47–56.
[51] M. Tichy, L. Lupínková, C. Sicora, I. Vass, S. Kuvikova, O. Prasil, J. Komenda, *Synechocystis* 6803 mutants expressing distinct forms of the Photosystem II D1 protein from *Synechococcus* 7942: relationship between the *psbA* coding region and sensitivity to visible and UV-B radiation, Biochim. Biophys. Acta 1605 (2003) 55–66.